

ON THE STABILITY OF SELF-GRAVITATING FILAMENTS

J. Freundlich¹, C. J. Jog², F. Combes¹ and S. Anathpindika²

Abstract. Filamentary structures are very common in astrophysical environments and are observed at various scales. On a cosmological scale, matter is usually distributed along filaments, and filaments are also typical features of the interstellar medium. Within a cosmic filament, matter can possibly contract and form galaxies, whereas an interstellar gas filament can clump into a series of bead-like structures which can then turn into stars. To investigate the growth of such instabilities and the properties of the resulting substructures, we consider idealized self-gravitating filaments and derive the dispersion relation for perturbations within them. We assume no specific density distribution, treat matter as a fluid, and use hydrodynamics to derive the linearized equations that govern the growth of perturbations. Assuming small local perturbations leads to a dispersion relation analogous to the spherical Jeans case: perturbations of size higher than the Jeans length collapse and asymmetries regarding their growth rates arise only because of rotation. For perturbations of arbitrary size, the dispersion relation retains its complex terms: all modes are potentially unstable, but elongated perturbations near the axis of the cylinder grow faster. Prolate substructures and global collapse are favored, which is corroborated by most observations of interstellar filaments.

Keywords: gravitation, hydrodynamics, instabilities, large-scale structure of the Universe, ISM: structure

1 Introduction

Although filaments have been observed since decades within molecular clouds (e.g., Schneider & Elmegreen 1979), cosmological simulations and high-resolution observations of the interstellar medium only recently showed the key role played by filamentary structures at various scales in astrophysics. Filamentary structures are indeed ubiquitous and involved in processes as varied as gas accretion onto galaxies and the formation of stars in the interstellar medium.

On cosmological scales, matter is usually distributed along filaments, forming a cosmic web that connects galaxies to one another (e.g., Bond et al. 1996) and provides a gas reservoir from which galaxies grow and accrete (e.g., Kere  et al. 2005; Dekel et al. 2009). The inner core of many of these filaments may be predominantly made of gas, as notably shown by simulations by Harford et al. (2008), motivating models which treat them as self-gravitating, isothermal or barotropic cylinders in hydrostatic equilibrium.

In the interstellar medium, observations show filamentary structures on much smaller scales (e.g., Andr  et al. 2010; Arzoumanian et al. 2011). Motivated by Herschel observations of star-forming environments, Andr  et al. (2010) suggest a scenario in which the formation of turbulence-driven filaments in the interstellar medium represents the first step towards core and star formation. The densest filaments would then fragment into pre-stellar cores owing to gravitational instability. Simulations reveal filamentary features arising either from turbulence (e.g., Padoan et al. 2001) or from intermediate stages of gravitational collapse (e.g., Gomez & Vazquez-Semadeni 2014).

2 Studying the growth of instabilities through linearized equations

The standard Jeans instability describes the collapse of a spherical gas cloud when the inner pressure is not strong enough to support the self-gravitating gas. The cylindrical case is more complicated and has not been fully investigated yet. Our goal is to obtain a dispersion relation for small perturbations arising in an idealized

¹ LERMA, Observatoire de Paris, CNRS, 61 av. de l'Observatoire, 75014 Paris, France

² Department of Physics, Indian Institute of Science, Bangalore 560012, India

filament in order to better understand the behavior of such perturbations, and to compare their properties with available observations and simulations. In order to do so, we derive the linearized dynamical equations that govern the perturbations and obtain the resulting dispersion relation, first for local perturbations within a rotating filament (section 3), and then for perturbations of any extent within a non-rotating filament (section 4).

Our idealized picture consists of an infinite self-gravitating cylinder with pressure and density related by a barotropic equation of state. We neglect the role of magnetic fields for simplicity, treat matter as an inviscid fluid and use hydrodynamics to obtain the linearized equations that govern the perturbations. Cylindrical symmetry involves no dependence on the axial and azimuthal coordinates z and ϕ for the unperturbed system, and we only consider axisymmetric perturbations. The unperturbed system is assumed to be at equilibrium, and we further assume that all fluid particles share the same initial axial velocity, $\vec{v}_0(R, \phi) = R\Omega_0(R) \vec{e}_\phi$, where $\Omega_0(R)$ is the undisturbed angular velocity, \vec{e}_ϕ the azimuthal unit vector and R the radial distance. The calculations are valid for any density profile $\rho_0(R)$, and the unperturbed gravitational field $\Phi_0(R)$ is set by the Poisson equation.

Assuming axisymmetric perturbations of the generic form $e^{-i\omega t} e^{ik_R R} e^{ik_z z}$ and introducing Oort constant $B(R) = -\frac{1}{2} [\Omega_0(R) + \frac{\partial}{\partial R} (R\Omega_0(R))]$, the dynamics of the perturbed system is determined by the following set of linearized first-order equations, where the infinitesimal disturbances are denoted by an index 1 while an index 0 corresponds to the unperturbed system (e.g., Mikhailovskii & Fridman 1973):

$$\omega v_{1R} - 2i\Omega_0 v_{1\phi} = -i \frac{\partial h_1}{\partial R} + k_R \Phi_1 \quad (2.1)$$

$$\omega v_{1\phi} - 2iB v_{1R} = 0 \quad (2.2)$$

$$\omega v_{1z} = k_z c_0^2 \frac{\rho_1}{\rho_0} + k_z \Phi_1 \quad (2.3)$$

$$\omega \rho_1 + i \frac{1}{R} \frac{\partial}{\partial R} (R \rho_0 v_{1R}) - k_z \rho_0 v_{1z} = 0 \quad (2.4)$$

$$\frac{1}{R} \frac{\partial}{\partial R} \left(R \frac{\partial \Phi_1}{\partial R} \right) - k_z^2 \Phi_1 = 4\pi G \rho_1. \quad (2.5)$$

These equations correspond respectively to the three projections of the equation of motion, the continuity equation, and the Poisson equation. The linearized barotropic equation of state yields for its part an enthalpy perturbation

$$h_1 = c_0^2 \frac{\rho_1}{\rho_0} \quad (2.6)$$

where $c_0(R)$ is the effective sound speed, defined by $c_0^2 = \partial p_0 / \partial \rho_0$ and potentially varying with radius. The pressure support could be thermal as well as turbulent.

3 Local perturbations in a rotating filament

We first assume local perturbations: the typical scale of the perturbation is small compared to that of the unperturbed quantities, i.e., $k_R R_0 \gg 1$, where R_0 is the typical radius for the unperturbed distribution. This assumption is analogous to the Wentzel-Kramers-Brillouin approximation (WKB) used in quantum physics and leads to the following local dispersion relation (Freundlich et al. 2014):

$$\omega^4 + \omega^2 (4\pi G \rho_0 - c_0^2 k^2 - \kappa^2) + \kappa^2 k_z^2 \left(c_0^2 - \frac{4\pi G \rho_0}{k^2} \right) = 0 \quad (3.1)$$

where $k = \sqrt{k_R^2 + k_z^2}$ corresponds to the total wavenumber and $\kappa(R)$ is the epicyclic frequency, defined by $\kappa^2 = -4\Omega_0 B$. $\rho_0(R)$ and $c_0(R)$ are respectively the initial density distribution and the effective sound speed.

This polynomial equation can be treated as a second order polynomial expression in ω^2 and it can be shown that its two roots ω_-^2 and ω_+^2 are real, with $\omega_-^2 < \omega_+^2$ and $\omega_+^2 \geq 0$. The system is thus globally stable to axisymmetric perturbations when $\omega_-^2 \geq 0$ and unstable when $\omega_-^2 < 0$, as growing modes require a non-zero imaginary part. Rotation generates asymmetries in the distribution of ω_-^2 in the phase plane (k_R, k_z) but the induced boundary between the stable and unstable regimes is symmetrical: the system is stable when $k^2 \geq k_{\text{crit}}$ with $k_{\text{crit}} = 4\pi G\rho_0/c_0^2$, and unstable below, which corresponds to the standard Jeans criterion. When there is no rotation, the dispersion relation further reduces to the standard dispersion relation for collapsing spherical systems. Figure 1 shows an illustrative example of the distribution of ω_-^2 for a rotating filament, where the asymmetries generated by rotation and the symmetrical boundary between stable and unstable regimes in the phase plane (k_R, k_z) are visible.

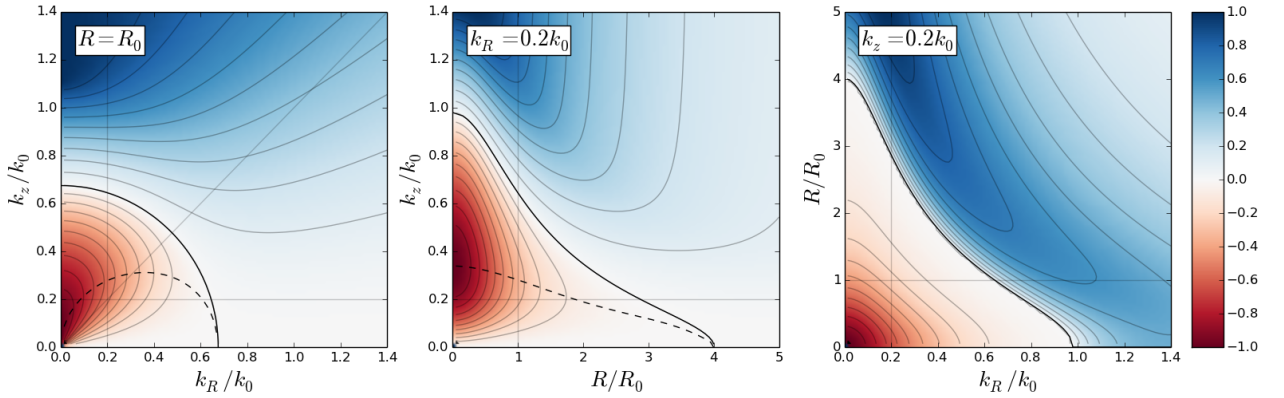


Fig. 1. As an illustrative example, we model a filament from the Taurus molecular cloud, TMC-1, with a Plummer-like density profile (Malinen et al. 2012) and plot the resulting distribution of ω_-^2 in the planes $R = R_0$, $k_R = 0.2k_0$, and $k_z = 0.2k_0$, where $k_0 = \sqrt{4\pi G\rho_c}/c_0$ is a characteristic wavenumber depending on the central density ρ_c . Negative values of ω_-^2 correspond to an unstable filament, and the solid black curve separates the stable and unstable regimes ($k = k_{\text{crit}}$). The dashed line corresponds to the minimum value of the frequency, i.e., to the most unstable mode.

4 Global perturbations in a non-rotating filament

The local WKB assumption prevents the perturbations feeling the large-scale geometry of the system and thus leads to the standard spherical Jeans case when there is no rotation. Releasing the WKB assumption should enable to better understand the specific effects of cylindrical geometry. Without this assumption and for non-rotating cylinders, the dispersion relation retains its complex terms and all modes are thus potentially unstable:

$$\omega^2 = -4\pi G\rho_0 \frac{k^2}{k^2 - i\frac{k_R}{R}} \left[1 - i\frac{k_R}{k^2} \left(\frac{1}{R} + \frac{1}{\rho_0} \frac{\partial \rho_0}{\partial R} \right) \right] + c_0^2 k^2 - ik_R \left[\frac{c_0^2}{R} + \frac{\partial c_0^2}{\partial R} \right] - \left[\frac{1}{R} + \frac{1}{\rho_0} \frac{\partial \rho_0}{\partial R} \right] \left[\frac{\partial c_0^2}{\partial R} - c_0^2 \frac{1}{\rho_0} \frac{\partial \rho_0}{\partial R} \right]. \quad (4.1)$$

Our previous calculations (Freundlich et al. 2014) included rotation. But although signs of rotation such as transverse velocity gradients are observed for interstellar filaments, and notably for TMC-1 in the Taurus molecular cloud (Olano et al. 1988), there generally does not seem to be a global coherent rotation of such filaments (e.g., Falgarone et al. 2001). This is why we restricted our calculations to non-rotating filaments here, as a first approximation.

As shown in Figure 2, this dispersion relation 4.1 shows that elongated perturbations near the axis of the filament grow faster, thus favoring elongated substructures. This is corroborated by observations, as most observations in the Taurus molecular cloud or in other molecular clouds favor prolate structures within interstellar filaments and tend to show that cores are stretched along the direction of the filaments (e.g., Curry 2002; Hartmann 2002).

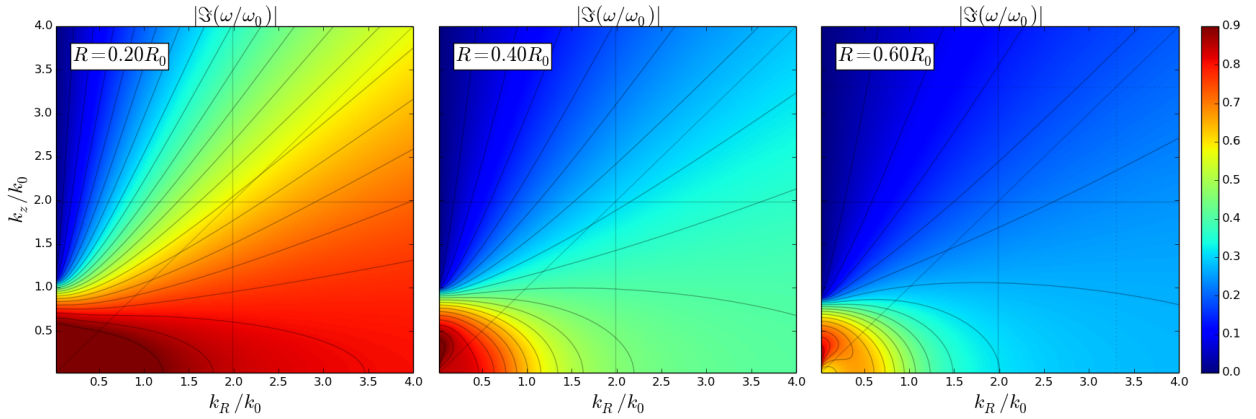


Fig. 2. Imaginary part of the angular frequency for an idealized filament inspired by TMC-1 in the phase plane (k_R , k_z) for three different radii, as derived from equation 4.1. The plotted quantity is a measure of the growth rate of the perturbations, thus prolate structures with $k_z < k_R$ are likely to be favored and we expect them to be more elongated nearest to the center of the filament, as shown by the change with radius of the isocontour lines.

5 Conclusion

We derived a dispersion relation for axisymmetric perturbations in infinite, self-gravitating, gaseous filaments in two different cases: (i) for perturbations of small extent when the filament is rotating (section 3), and (ii) for perturbations of any extent when the filament is not rotating (section 4). The gas is assumed to be barotropic, and the relations are valid for any type of density profile. In the first case, perturbations of size higher than the Jeans length collapse and asymmetries only arise because of rotation, whereas in the second case, all modes are potentially unstable but elongated perturbations near the axis of the cylinder grow faster, which is corroborated by most observations of interstellar filaments.

Our model assumes an infinite and isolated filament, but we could generalize our calculations to a cylinder of finite size and take into account the effects of the environment and of more complex velocity distributions. This work should be complemented by more detailed comparisons with observations and by numerical studies of the formation and subsequent collapse of idealized filaments, which we plan to do in future studies.

This work benefited from the European Research Council Advanced Grant Program number 267399 - Momentum, and J. F. acknowledges support from the Indo French Center for the Promotion of Advanced Research (IFCPAR/CEFIPRA) through a Raman-Charpak fellowship.

References

- André, P., Mouschikoff, A., Bontemps, S., et al. 2010, *A&A*, 518, 102
 Arzoumanian, D., André, P., Didelon, P., et al. 2011, *A&A*, 529, 6
 Bond, J. R., Kofman, L., & Pogosyan, D. 1996, *Nature*, 380, 603
 Curry, C. L. 2002, *ApJ*, 576, 849
 Dekel, A., Birnboim, Y., Engel, G., et al. 2009, *Nature*, 457, 451
 Falgarone, E., Pety, J., & Phillips, T. G. 2001, *ApJ*, 555, 178
 Freundlich, J., Jog, C. J., & Combes, F. 2014, *A&A*, 564, 7
 Gomez, G. C. & Vazquez-Semadeni, E. 2014, submitted to *ApJ* [arXiv:1308.6298]
 Harford, A. G., Andrew, J. S., & Gnedin, N. Y. 2008, *MNRAS*, 389, 880
 Hartmann, L. 2002, *ApJ*, 578, 914
 Kereš, D., Katz, N., Weinberg, D. H., & Davé, R. 2005, *MNRAS*, 363, 2
 Malinen, J., Juvela, M., Rawlings, M. G., et al. 2012, *A&A*, 544, 50
 Mikhailovskii, A. B. & Fridman, A. M. 1973, *Soviet Physics - JETP*, 17, 57
 Olano, C. A., Walmsley, C. M., & Wilson, T. L. 1988, *A&A*, 196, 194
 Padoan, P., Juvela, M., Goodman, A. A., & Nordlund, Å. 2001, *ApJ*, 553, 227
 Schneider, S. & Elmegreen, B. G. 1979, *ApJS*, 41, 87